Journal of Sound and Vibration (2001) **247**(4), 561–576
doi:10.1006/jsvi.2001.3689, available online at http://www.idealibrary.com on IDEAL®

ACTIVE STRUCTURAL CONTROL BASED ON THE PREDICTION AND DEGREE OF STABILITY

U. ALDEMIR

Faculty of Civil Engineering, Division of Applied Mechanics, Istanbul Technical University, 80626 Maslak, Istanbul, Turkey. E-mail: aldemiru@itu.edu.tr

AND

M. BAKIOGLU

Faculty of Civil Engineering, Division of Applied Mechanics, Istanbul Technical University, 80626 Maslak, Istanbul, Turkey

(*Received* 6 *March* 2000, *and in final form* 5 *February* 2001)

Active control of buildings and structures for reducing damage due to earthquake and other environmental forces represents a relatively new research area. Most of the recent studies on this area are based on the applications of traditional linear quadratic regulator (LQR) control to the earthquake-excited structures. This paper presents the analytical solution of the modified linear quadratic regulator (MLQR) problem including a parameter α known as system stability order in the presence of unknown seismic excitation. The resulting closed–open loop active control force depends on the system state, seismic excitation and α. An approximate solution of the problem is based on the real-time prediction of near-future excitation. Since the primary focus of this study is on the relation between the system stability order α and the prediction of near-future excitation, numerical simulations of a three-storey undamped structure subjected to an El Centro earthquake are performed for different α values. It is shown that the relative displacements can be reduced significantly for each selected α value as the near-future excitation is predicted precisely and there is no significant increase in the control forces. The results also show that there is no need to predict the distant-future excitation to be able to achieve a given reduction in relative displacements as the system stability order α is increased. It is also shown that the accelerations increase in general after the fourth-step ahead prediction for a given α while they decrease as α increases.

1. INTRODUCTION

Active control of structures for earthquake hazard mitigation has been the subject of considerable research since the pioneer work of Yao [1]. Several different active control algorithms have been proposed in the past three decades. Recent developments in the subject have been extensively reviewed by Soong [2] and Housner *et al.* [3].

Determination of the active control force is based on the minimization of a given performance index with respect to the control force under the constraint conditions defined by the equation of motion and the initial conditions. Once the performance index has been selected, its minimization can be performed by using the minimum principle of Pontryagin [4] or the method of dynamic programming of Bellman [5]. In the first approach, which is a variational principle, optimal control is derived by minimizing a given function known as the Hamiltonian. In practice, the admissible control forces are bounded and there is a limit

0022-460X/01/440561 + 16 $35.00/0

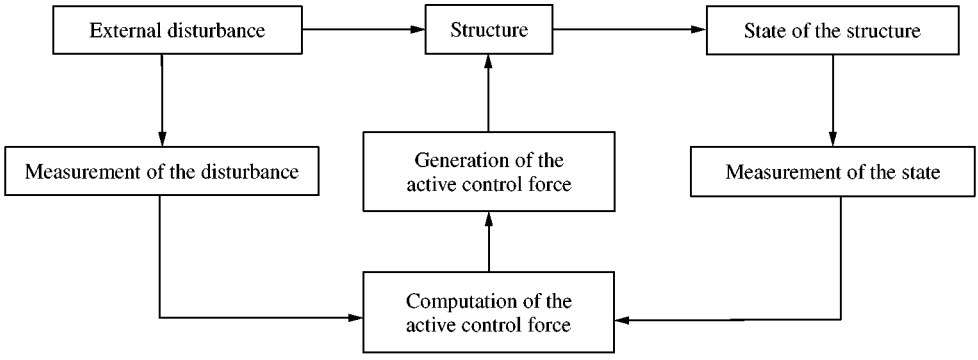

Figure 1. Schematic representation of active structural control system.

on their magnitudes. This approach is applicable to control problems with constraints on the admissible control forces. The second approach uses the principle of optimality, which states that a control policy that is optimal over the whole control interval is also optimal over all subintervals. With few exceptions, since the solution of equations in the second approach is more difficult compared to the first approach it has been suggested to use the second approach as a check for sufficiency. The second approach is widely used in the optimization of discrete, multi-stage systems. Both approaches are complementary tools for the solutions of the optimal control problems even though they result in the same conditions for many problems. However, one formulation may be better than the other to solve a particular problem.

A basic configuration of an active control system is shown schematically in Figure 1. Classical active control algorithms in which the quadratic performance index is defined as an integral function of the system response and control force over the whole control interval have been widely used in structural active control applications. These algorithms can be classified as closed-loop, open-loop and closed–open loop. In closed-loop control, active control force is regulated by the state vector which is the response of the structure. If the computation of the active control force requires only the seismic excitation information, then this control algorithm can be considered as open-loop. When the state vector and the external excitation are used in the computation of the active control force, this results in a closed–open loop control algorithm.

Among these three algorithms, only a classical closed-loop algorithm is applicable to earthquake-excited structures. However, since it requires the earthquake excitation to vanish within the control interval defined as a time duration in which the control process is executed or to be a white noise stochastic process, which is not realistic in most cases, it does not satisfy the optimality condition. On the other hand, even though the classical closed–open loop and open-loop control algorithms are superior to the closed-loop control, since their solutions require the whole knowledge of the external seismic excitation which is not known *a priori*, they are not applicable to structures subjected to seismic forces.

In the past decade, Yang *et al.* [6, 7], Masri *et al.* [8], Rodellar *et al.* [9] and Lee and Kozin [10] have made excellent contributions to overcome this deficiency of the classical active control algorithms. In addition to these methods, active control of structures has been investigated as a tracking problem using dynamic programming [11]. Iemura *et al.* [12] have also proposed a new closed–open loop control based on the stochastic control theory in which an energy-based stochastic criterion is employed by considering the structure and the ground as a single system. Another instantaneous closed–open loop

control that takes into account the seismic energy input to the structure has been developed in reference [13]. Aldemir and Bakioglu [14] proposed a semiactive closed–open loop control algorithm by forcing the rate of change of the system energy to be as negative as possible.

It is known that the system stability is determined by the real parts of the eigenvalues of the closed-loop control system. If all the eigenvalues have negative real parts, the solution approaches the equilibrium point as time increases, so that the solution is asymptotically stable. In one particular case, if all the eigenvalues have negative real parts less than some negative real number $-\alpha$, $\alpha > 0$, then it is said that the system as a degree of stability $-\alpha$ [15]. These types of systems with a certain stability order $-\alpha$ can be designed easily by using LQR theory.

This paper derives the analytical solution of the modified linear quadratic regulator (MLQR) problem including the system stability order $-\alpha$ without ignoring the unknown disturbance while the standard LQR problem corresponds to a special case of the MLQR problem in which $\alpha = 0$. The resulting active control force depends on the state vector, external excitation and the stability order α which has a contribution to the control force in both feed-forward and feed-back terms. Approximate solution of the closed–open loop control is carried out by considering the near-future excitation influence. In a numerical example, responses of a three-storey lumped mass undamped structure with different α values are examined to investigate the relation between the stability order α and the near-future excitation. Numerical results show that the reduction in the relative displacements will increase independently from the stability order α as the more distant-future excitation is predicted precisely. The significance of each predicted earthquake acceleration value in the solution increases as the system stability order α is increased. Therefore, a given performance in terms of the reduction in relative displacements can be achieved by predicting less near-future excitation values for higher values of α. Numerical results for the peak values of the storey accelerations show that the accelerations decrease as the stability order α increases while they increase in general after the fourth-step ahead prediction for a given α.

2. THEORY

2.1. BUILDING MODEL

A linear building structure modelled by an n-degree-of-freedom lumped mass–spring–dash pot system subjected to a horizontal earthquake ground acceleration $\ddot{x}_g(t)$ and the control $\mathbf{U}(t)$ is shown in Figure 2. In the idealized model, the lumped mass approach in which the mass of the structure is assumed to be concentrated at floor levels is used. The columns of the building are assumed to be massless and modelled as a linear elastic spring with a linear dash pot in parallel. The control is implemented by means of the actuators installed in every storey unit and instead of the actuators, the actuator control forces are shown in Figure 2. For the purpose of deriving the equations of motion, a free-body diagram of the ith storey is given in Figure 3.

The equation of motion for the ith storey can be written as

$$m_i\ddot{x}_i - c_i\dot{x}_{i-1} + (c_i + c_{i+1})\dot{x}_i - c_{i+1}\dot{x}_{i+1} - k_i x_{i-1} + (k_i + \mathrm{k}_{i+1})x_i$$

$$- k_{i+1}x_{i+1} = -m_i\ddot{x}_g(t) + u_{i+1} - u_i, \tag{1}$$

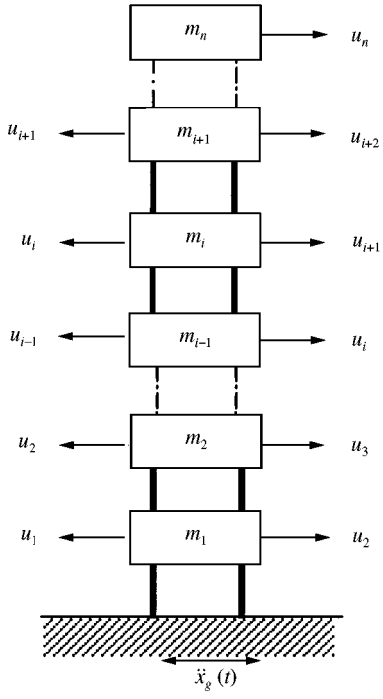

Figure 2. Idealized structural model.

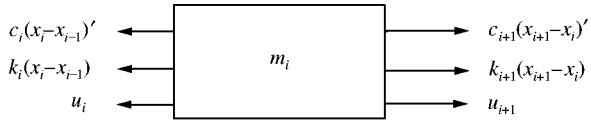

Figure 3. Free-body diagram for the ith storey.

where m_i, x_i, k_i, c_i, u_i, $(i = 1, \ldots, n)$ are the mass, relative displacement with respect to the ground, linear elastic stiffness coefficient, linear viscous damping coefficient and the control force for the ith storey respectively. It is assumed that the relative displacements (x_i), velocities $(\dot{x}_i)$ and the ground accelerations $(\ddot{x}_g(t))$ can be measured in real time by the sensors installed in every storey unit. If equation (1) is restated for $i = 1, \ldots, n$, then the governing equations of motion are derived as follows:

$$m_1\ddot{x}_1 + (c_1 + c_2)\dot{x}_1 - c_2\dot{x}_2 + (k_1 + k_2)x_1 - k_2x_2 = -m_1\ddot{x}_g(t) + u_2 - u_1,$$

$$m_2\ddot{x}_2 - c_2\dot{x}_1 + (c_2 + c_3)\dot{x}_2 - c_3\dot{x}_3 - k_2x_1 + (k_2 + k_3)x_2 - k_3x_3 = -m_2\ddot{x}_g(t) + u_3 - u_2,$$

$$\vdots$$

$$m_n\ddot{x}_n - c_n\dot{x}_{n-1} + c_n\dot{x}_n - k_nx_{n-1} + k_nx_n = -m_n\ddot{x}_g(t) - u_n. \tag{2}$$

Using the matrix–vector notation, the system of equations given above in discrete form can also be expressed as

$$\mathbf{M}\ddot{\mathbf{X}}(t) + \mathbf{K}\mathbf{X}(t) + \mathbf{C}\dot{\mathbf{X}}(t) = \mathbf{m}\ddot{x}_g(t) + \mathbf{L}\mathbf{U}(t), \tag{3}$$

where $\mathbf{X}(t) = [x_1, x_2, \ldots, x_n]^T$ is the n-dimensional response vector denoting the relative displacements (here T indicates the transpose of vector and matrix); $\mathbf{M}$, $\mathbf{C}$ and $\mathbf{K}$ are $(n \times n)$-dimensional positive-definite matrices corresponding to the mass, viscous damping and the stiffness of the structure, respectively; $\mathbf{m} = -[m_1, m_2, \ldots, m_n]^T$; $\mathbf{L}$ is the $(n \times n)$-dimensional location matrix of n controllers; $\mathbf{U}(t)$ is the n-dimensional active control force vector. The matrices $\mathbf{M}$, $\mathbf{K}$, $\mathbf{C}$ and $\mathbf{L}$ are of the following form:

$$\mathbf{M} = \begin{bmatrix} m_1 & & & & 0 \\ & m_2 & & & \\ & & m_3 & & \\ & & & \cdot & \\ 0 & & & & m_n \end{bmatrix}; \quad \mathbf{K} = \begin{bmatrix} k_1 + k_2 & -k_2 & & & \\ -k_2 & k_2 + k_3 & -k_3 & & 0 \\ & -k_3 & \cdot & \cdot & \\ & & \cdot & \cdot & -k_{n-1} \\ & 0 & & -k_{n-1} & k_{n-1} + k_n \quad -k_n \\ & & & & -k_n \quad k_n \end{bmatrix} \tag{4}$$

$$\mathbf{C} = \begin{bmatrix} c_1 + c_2 & -c_2 & & & \\ -c_2 & c_2 + c_3 & -c_3 & & 0 \\ & -c_3 & \cdot & \cdot & \\ & & \cdot & \cdot & -c_{n-1} \\ & 0 & & -c_{n-1} & c_{n-1} + c_n \quad -c_n \\ & & & & -c_n \quad c_n \end{bmatrix}; \quad \mathbf{L} = \begin{bmatrix} -1 & 1 & & & \\ & -1 & 1 & & 0 \\ & & \cdot & \cdot & \\ & & & \cdot & \cdot \\ & 0 & & -1 & 1 \\ & & & & -1 \end{bmatrix}.$$

Now, in order to formulate the optimal controller, equation (3) can be expressed in a state-space form as

$$\dot{\mathbf{Z}} = \mathbf{A}\mathbf{Z} + \mathbf{B}\mathbf{U} + \mathbf{H}\ddot{x}_g(t), \quad \mathbf{Z}(0) = \mathbf{0}, \tag{5}$$

where

$$\mathbf{Z}(t) = \begin{bmatrix} \mathbf{X}(t) \\ \dot{\mathbf{X}}(t) \end{bmatrix}, \quad \mathbf{A} = \begin{bmatrix} \mathbf{0} & \mathbf{I} \\ -\mathbf{M}^{-1}\mathbf{K} & -\mathbf{M}^{-1}\mathbf{C} \end{bmatrix}, \quad \mathbf{B} = \begin{bmatrix} \mathbf{0} \\ \mathbf{M}^{-1}\mathbf{L} \end{bmatrix}, \quad \mathbf{H} = \begin{bmatrix} \mathbf{0} \\ \mathbf{M}^{-1}\mathbf{m} \end{bmatrix}. \tag{6}$$

Optimal active control law is derived by the minimization of the performance measure J_α, a modification to the classical quadratic performance index [15],

$$J_\alpha = \int_0^t e^{2\alpha t} \, (\mathbf{Z}^T\mathbf{Q}\mathbf{Z} + \mathbf{U}^T\mathbf{R}\mathbf{U}) \, dt, \tag{7}$$

where t_1 is a duration defined to be longer than that of the earthquake ground acceleration; α is a positive number which represents the stability order of the system, $\mathbf{Q}$ is a $(2n \times 2n)$ dimensional positive semidefinite symmetric weighting matrix for the structure response, and $\mathbf{R}$ is an $(n \times n)$ dimensional positive definite symmetric weighting matrix for the control force. As long as the performance-measure matrices $\mathbf{Q}$ and $\mathbf{R}$ are selected as positive semidefinite and positive definite, respectively, the resulting optimal solution will be asymptotically stable. Numerical values for the elements of $\mathbf{Q}$ and $\mathbf{R}$ matrices are assigned according to the relative importance of the state variables and the control forces in the minimization procedure in order to adjust the power requirements in the actuators. If it is

required to achieve a significant decrease in structure response in time domain, larger values must be assigned to the elements of the weighting matrix $\mathbf{Q}$ than those of the weighting matrix $\mathbf{R}$. Some approximate rules for the selection of these performance-measure matrices can be found in references [2, 16].

2.2. ANALYTICAL SOLUTION OF THE MLQR PROBLEM

For the solution of the MLQR problem given by equations (5) and (7), it is necessary to express the problem in standard LQR form. For this purpose, introduce the variables

$$\boldsymbol{\varsigma}(t) = \mathrm{e}^{\alpha t}\mathbf{Z}(t);\ \mathbf{v}(t) = \mathrm{e}^{\alpha t}\mathbf{U}(t). \tag{8}$$

Using these new variables, equations (5) and (7) can be rewritten as

$$\dot{\boldsymbol{\varsigma}}(t) = \bar{\mathbf{A}}\boldsymbol{\varsigma}(t) + \mathbf{B}\mathbf{v}(t) + \bar{\mathbf{f}}(t);\ \boldsymbol{\varsigma}(0) = \mathbf{0}, \tag{9}$$

$$J_\alpha = \int_0^{t_1} (\boldsymbol{\varsigma}^{\mathrm{T}}\mathbf{Q}\boldsymbol{\varsigma} + \mathbf{v}^{\mathrm{T}}\mathbf{R}\mathbf{v})\,\mathrm{d}t, \tag{10}$$

where $\bar{\mathbf{A}} = \mathbf{A} + \alpha\mathbf{I}$ and $\bar{\mathbf{f}}(t) = \mathrm{e}^{\alpha t}\mathbf{H}\ddot{x}_g(t)$. It should be noted here that the new variable $\boldsymbol{\varsigma}(t)$ is not the actual state of the system. So, upon solving the standard LQR problem given by equations (9) and (10), the resulting solution must be expressed in terms of the actual state $\mathbf{Z}(t)$ and the actual control force $\mathbf{U}(t)$ to be able to interpret the behaviour of the structure under the proposed control easily. Firstly, the optimal active control force $\mathbf{U}(t)$ will be found and then substituted into equation (5) to get the closed-loop system. As explained in section 1, if all the eigenvalues of the closed-loop system matrix have negative real parts, then the system under the proposed control is asymptotically stable.

Analytical solution of the linear regulator problem is derived generally by using Pontryagin's minimum principle which gives the necessary condition of optimality, but in general it is not a sufficient condition. Defining the Hamiltonian

$$H = \boldsymbol{\varsigma}^{\mathrm{T}}\mathbf{Q}\boldsymbol{\varsigma} + \mathbf{v}^{\mathrm{T}}\mathbf{R}\mathbf{v} + \boldsymbol{\lambda}^{\mathrm{T}}[\bar{\mathbf{A}}\boldsymbol{\varsigma}(t) + \mathbf{B}\mathbf{v}(t) + \mathrm{e}^{\alpha t}\mathbf{H}\ddot{x}_g(t)] \tag{11}$$

optimality conditions to be satisfied are obtained as follows:

$$\dot{\boldsymbol{\varsigma}}(t) = \frac{\partial H}{\partial \boldsymbol{\lambda}} = \bar{\mathbf{A}}\boldsymbol{\varsigma}(t) + \mathbf{B}\mathbf{v}(t) + \mathrm{e}^{\alpha t}\mathbf{H}\ddot{x}_g(t), \quad \boldsymbol{\varsigma}(0) = \mathbf{0}, \tag{12}$$

$$\dot{\boldsymbol{\lambda}} = -\frac{\partial H}{\partial \boldsymbol{\zeta}} = -2\mathbf{Q}\boldsymbol{\varsigma}(t) - \bar{\mathbf{A}}^{\mathrm{T}}\boldsymbol{\lambda}(t), \quad \boldsymbol{\lambda}(t_1) = \mathbf{0}, \tag{13}$$

$$\frac{\partial H}{\partial \mathbf{v}} = \mathbf{0} = 2\mathbf{R}\mathbf{v}(t) + \mathbf{B}^{\mathrm{T}}\boldsymbol{\lambda}(t), \tag{14}$$

where $\boldsymbol{\lambda}(t)$ is a $2n$ vector of Lagrangian multipliers. Depending on the type of $\boldsymbol{\lambda}(t)$, closed-loop, open-loop and closed–open loop control laws can easily be derived. For the closed–open loop solution, assume that $\boldsymbol{\lambda}(t)$ has the form

$$\boldsymbol{\lambda}(t) = \mathbf{P}(t)\boldsymbol{\varsigma}(t) + \mathbf{r}(t). \tag{15}$$

Inserting $\boldsymbol{\lambda}(t)$ and $\dot{\boldsymbol{\lambda}}(t)$ in terms of $\mathbf{P}(t)$, $\boldsymbol{\varsigma}(t)$ and $\mathbf{r}(t)$ into equations (12)–(14), gives the following equation:

$$[\dot{\mathbf{P}}(t) + \mathbf{P}(t)\bar{\mathbf{A}} - \tfrac{1}{2}\mathbf{P}(t)\mathbf{B}\mathbf{R}^{-1}\mathbf{B}^{\mathrm{T}}\mathbf{P}(t) + \bar{\mathbf{A}}^{\mathrm{T}}\mathbf{P}(t) + 2\mathbf{Q}]\boldsymbol{\varsigma}(t)$$

$$+ \dot{\mathbf{r}}(t) - [\tfrac{1}{2}\mathbf{P}(t)\mathbf{B}\mathbf{R}^{-1}\mathbf{B}^{\mathrm{T}} - \bar{\mathbf{A}}^{\mathrm{T}}]\mathbf{r}(t) + \mathbf{P}(t)\mathbf{H}e^{\alpha t}\ddot{x}_g(t) = \mathbf{0}. \tag{16}$$

Equation (16) can be satisfied for all times if and only if the equations

$$\dot{\mathbf{P}}(t) + \mathbf{P}(t)\bar{\mathbf{A}} - \tfrac{1}{2}\mathbf{P}(t)\mathbf{B}\mathbf{R}^{-1}\mathbf{B}^{\mathrm{T}}\mathbf{P}(t) + \bar{\mathbf{A}}^{\mathrm{T}}\mathbf{P}(t) + 2\mathbf{Q} = \mathbf{0}, \quad \mathbf{P}(t_1) = \mathbf{0}, \tag{17}$$

$$\dot{\mathbf{r}}(t) - [\tfrac{1}{2}\mathbf{P}(t)\mathbf{B}\mathbf{R}^{-1}\mathbf{B}^{\mathrm{T}} - \bar{\mathbf{A}}^{\mathrm{T}}]\mathbf{r}(t) + \mathbf{P}(t)\mathbf{H}e^{\alpha t}\ddot{x}_g(t) = \mathbf{0}, \quad \mathbf{r}(t_1) = \mathbf{0} \tag{18}$$

are valid. Optimal closed–open loop control force $\mathbf{v}(t)$ is derived from equations (14) and (15) as in the following form:

$$\mathbf{v}(t) = -\tfrac{1}{2}\mathbf{R}^{-1}\mathbf{B}^{\mathrm{T}}[\mathbf{P}(t)\boldsymbol{\varsigma}(t) + \mathbf{r}(t)]. \tag{19}$$

For closed-loop control equation (19) becomes

$$\mathbf{v}(t) = -\tfrac{1}{2}\mathbf{R}^{-1}\mathbf{B}^{\mathrm{T}}\mathbf{P}(t)\boldsymbol{\varsigma}(t). \tag{20}$$

Using the transformations given by equation (8), equation (19) can be rewritten in terms of $\mathbf{Z}(t)$ and $\mathbf{U}(t)$ as

$$\mathbf{U}(t, \mathbf{Z}) = -\tfrac{1}{2}\mathbf{R}^{-1}\mathbf{B}^{\mathrm{T}}(e^{\alpha t}\mathbf{r} + \mathbf{P}\mathbf{Z}). \tag{21}$$

Equations (18) and (21) can also be expressed as

$$\dot{\boldsymbol{\varphi}} - \mathbf{E}\boldsymbol{\varphi} + \mathbf{P}\mathbf{H}\ddot{x}_g(t) = \mathbf{0}; \ \boldsymbol{\varphi}(t_1) = \mathbf{0}, \tag{22}$$

$$\mathbf{U}(t, \mathbf{Z}) = -\tfrac{1}{2}\mathbf{R}^{-1}\mathbf{B}^{\mathrm{T}}(\boldsymbol{\varphi} + \mathbf{P}\mathbf{Z}), \tag{23}$$

where

$$\boldsymbol{\varphi}(t) = e^{-\alpha t}\mathbf{r}; \ \mathbf{E} = \tfrac{1}{2}\mathbf{P}\mathbf{B}\mathbf{R}^{-1}\mathbf{B}^{\mathrm{T}} - \bar{\bar{\mathbf{A}}}^{\mathrm{T}}; \ \bar{\bar{\mathbf{A}}} = \mathbf{A} + 2\alpha\mathbf{I}. \tag{24}$$

In equation (23), the coefficient of $\mathbf{Z}$ is called feed-back term and the rest is called feed-forward term. Consequently, optimal control force which minimizes the performance function given by equation (7) under the constraint given by equation (5) can be calculated by equation (23) such that $\mathbf{P}$ and $\boldsymbol{\varphi}$ are the solutions of equations (17) and (22). If equation (23) is substituted into equation (5), then the equation which describes the behaviour of the structure under optimal closed–open loop control is given as

$$\dot{\mathbf{Z}} = \tilde{\mathbf{A}}\mathbf{Z} + \bar{\boldsymbol{\varphi}}(t), \quad \mathbf{Z}(0) = \mathbf{0}, \tag{25}$$

where

$$\tilde{\mathbf{A}} = \mathbf{A} - \tfrac{1}{2}\mathbf{B}\mathbf{R}^{-1}\mathbf{B}^{\mathrm{T}}\mathbf{P}; \quad \bar{\boldsymbol{\varphi}}(t) = -\tfrac{1}{2}\mathbf{B}\mathbf{R}^{-1}\mathbf{B}^{\mathrm{T}}\boldsymbol{\varphi} + \mathbf{H}\ddot{x}_g(t). \tag{26}$$

3. NUMERICAL SOLUTION

Solution of the closed–open loop optimal control problem formulated as the MLQR problem is reduced to the solution of the first order matrix differential equations and derived by using the Taylor Series method. The MLQR problem requires the solutions of

three matrix differential equations for $\mathbf{P}(t)$, $\boldsymbol{\varphi}(t)$ and $\mathbf{Z}(t)$ given by equations (17), (22) and (25) respectively. The solution of the matrix Riccati equation which does not include the excitation term $\ddot{x}_g(t)$ approaches a constant value after a short time [2] in structural control applications. So, it is generally solved as an algebraic equation by neglecting the derivative term. However, backward solution of equation (22) requires a prior knowledge of the earthquake excitation in $[0, t_1]$, which is not possible. Approximate solution forward in time for $\boldsymbol{\varphi}(t)$ will be carried out including the near-future influence of the earthquake excitation. Once the solutions for $\mathbf{P}(t)$ and $\boldsymbol{\varphi}(t)$ are obtained, the forward solution of equation (25) can easily be obtained.

For the derivation of the backward solution of equation (22), firstly assume that it has an initial condition $\boldsymbol{\varphi}_0$ at $t = 0$ as given below:

$$\dot{\boldsymbol{\varphi}}(t) = \mathbf{E}\boldsymbol{\varphi}(t) + \mathbf{l}(t), \quad \boldsymbol{\varphi}(0) = \boldsymbol{\varphi}_0, \tag{27}$$

where the non-homogeneous term

$$\mathbf{l}(t) = -\mathbf{PH}\ddot{x}_g(t). \tag{28}$$

Equation (24) shows that $\mathbf{E}$ matrix is a constant matrix since the Riccati matrix $\mathbf{P}(t)$ is assumed to be constant. Then, the complete solution of equation (27) is the sum of the homogeneous solution and the particular solution and given by [17]

$$\boldsymbol{\varphi}(t) = \mathrm{e}^{\mathbf{E}t}\boldsymbol{\varphi}(0) + \int_0^t \mathrm{e}^{\mathbf{E}(t-\tau)}\mathbf{l}(\tau)\,\mathrm{d}\tau. \tag{29}$$

The $\boldsymbol{\varphi}$ vector at the kth point, $\boldsymbol{\varphi}_k$ can be calculated by using Taylor Series method, in terms of $\boldsymbol{\varphi}_0$ as

$$\boldsymbol{\varphi}_k = \mathbf{S}^k\boldsymbol{\varphi}_0 + \sum_{i=1}^{k} \mathbf{S}^{k-i}\mathbf{p}_i, \tag{30}$$

where

$$\mathbf{S} = \mathbf{I} + h\mathbf{E} + \frac{1}{2!}h^2\mathbf{E}^2 + \frac{1}{3!}h^3\mathbf{E}^3 + \frac{1}{4!}h^4\mathbf{E}^4, \tag{31}$$

$$\mathbf{p}_{j+1} = h\left(\mathbf{I} + \frac{1}{2}h\mathbf{E} + \frac{1}{6}h^2\mathbf{E}^2 + \frac{1}{24}h^3\mathbf{E}^3 + \frac{1}{120}h^4\mathbf{E}^4\right)\mathbf{l}_j + h\left(\frac{1}{2}\mathbf{I} + \frac{1}{6}h\mathbf{E} + \frac{1}{24}h^2\mathbf{E}^2 + \frac{1}{120}h^3\mathbf{E}^3 + \frac{1}{710}h^4\mathbf{E}^4\right)(\mathbf{l}_{j+1} - \mathbf{l}_j). \tag{32}$$

However, the terminal condition for $\boldsymbol{\varphi}$ is given at time $t_1 = mh$ as $\boldsymbol{\varphi}(t_1) = \boldsymbol{\varphi}_m = \mathbf{0}$. Here, m and h denote the number of equal intervals and the time step, respectively, in the control interval $[0, t_1]$. Using the condition $\boldsymbol{\varphi}(t_1) = \boldsymbol{\varphi}_m = \mathbf{0}$, $\boldsymbol{\varphi}_0$ can be obtained from equation (30) as follows:

$$\boldsymbol{\varphi}_0 = -\sum_{i=1}^{m} \mathbf{S}^{-i}\mathbf{p}_i. \tag{33}$$

Substituting $\boldsymbol{\varphi}_0$ given by equation (33) into equation (30) and writing equation (30) for any point j results in the following equation:

$$\boldsymbol{\varphi}_j = -\sum_{i=j+1}^{m} \mathbf{S}^{j-i}\mathbf{p}_i = -\mathbf{S}^{-1}\mathbf{p}_{j+1} - \mathbf{S}^{-2}\mathbf{p}_{j+2} - \cdots - \mathbf{S}^{j-m}\mathbf{p}_m. \tag{34}$$

Equation (34) shows that $\boldsymbol{\varphi}_j$ values at any point j can be calculated only if the $\mathbf{p}_i(\mathbf{i} > j)$ terms, which are completely beyond the point j, are known *a priori*. $\mathbf{p}_i(\mathbf{i} > j)$ terms cannot be known *a priori* since they include the unknown excitation terms. However, their near-future values can be predicted by using their known values in the past. Details of the prediction process are given in reference [18]. If the sound norm of the matrix $\mathbf{S}^{j-i}$ $(j - i < 0)$, $(\|\mathbf{S}^{j-i}\|_2 = \rho_{min}^{1/2}[(\mathbf{S}^{j-i})^{\mathrm{T}}\mathbf{S}^{j-i}]$ where $\rho_{min}[(\mathbf{S}^{j-i})^{\mathrm{T}}\mathbf{S}^{j-i}]$ denotes the maximum eigenvalue of the matrix $[(\mathbf{S}^{j-i})^{\mathrm{T}}\mathbf{S}^{j-i}]$) decreases sharply with the increasing i, including the near-future excitation influence in the solution gives a good approximation to optimal solution [18].

4. NUMERICAL EXAMPLE

The primary focus of this paper is on the relationship between the stability order α and the near-future excitation. For this purpose, the peak storey relative displacements, accelerations and the control forces of a three-storey undamped structure are examined for different α values. Firstly, the results for the standard LQR ($\alpha = 0$) case and then the results for MLQR control are presented. Using the idealized description of the n-degree-of-freedom structure given in Figure 2, the example structure is characterized by the following system matrix $\mathbf{A}$:

$$\mathbf{A} = \begin{bmatrix} \mathbf{0} & \mathbf{I} \\ -\mathbf{M}^{-1}\mathbf{K} & -\mathbf{M}^{-1}\mathbf{C} \end{bmatrix} = \begin{bmatrix} & \mathbf{0}_3 & & \mathbf{I}_3 \\ -1{\cdot}8375 & 0{\cdot}8704 & 0 & \\ 0{\cdot}8704 & -1{\cdot}3540 & 0{\cdot}4835 & \mathbf{0}_3 \\ 0 & 0{\cdot}4835 & -0{\cdot}4835 & \end{bmatrix}, \tag{35}$$

where $\mathbf{0}_3$ and $\mathbf{I}_3$ are (3×3) zero and identity matrices. The weighting matrix $\mathbf{R}(3 \times 3)$ for the active control force and the weighting matrix $\mathbf{Q}(6 \times 6)$ for the structure response are selected as follows:

$$\mathbf{R} = \begin{bmatrix} 1 & 0 & 0 \\ 0 & 1 & 0 \\ 0 & 0 & 1 \end{bmatrix} * 10^{-5}, \quad \mathbf{Q} = \begin{bmatrix} 10{\cdot}5 & 7{\cdot}875 & 4{\cdot}2 & 10{\cdot}5 & 7{\cdot}875 & 4{\cdot}2 \\ & 7{\cdot}35 & 4{\cdot}2 & 7{\cdot}875 & 7{\cdot}35 & 4{\cdot}2 \\ & & 3{\cdot}675 & 4{\cdot}2 & 4{\cdot}2 & 3{\cdot}675 \\ & & & 10{\cdot}5 & 7{\cdot}875 & 4{\cdot}2 \\ & \text{symm} & & & 7{\cdot}35 & 4{\cdot}2 \\ & & & & & 3{\cdot}675 \end{bmatrix}. \tag{36}$$

The weighting matrix $\mathbf{R}(3 \times 3)$ is a positive-definite matrix since its all eigenvalues are positive. The weighting matrix $\mathbf{Q}(6 \times 6)$ is a positive semi-definite matrix since it has three zero eigenvalues and three positive eigenvalues; 1·0999, 3·5343, 38·4158. The 1940 El Centro ground motion which is one of the earliest recorded and most widely used near-field ground motions is used to excite the structure. The acceleration history of the North–South El Centro ground motion is shown in Figure 4. Dynamic responses of the example structure subjected to El Centro ground motion which is shown in Figure 4 have been investigated for the cases consisting of uncontrolled, closed-loop control, optimal closed–open loop control with known earthquake time history and approximate closed–loop control with near-future earthquake excitation influence for $\alpha = 0$ case.

Relative displacements of the first and the third floor for the first 10 s which include the peak values are shown in Figures 5 and 6 for the cases of optimal closed–open loop assuming that the earthquake excitation is known *a priori* and approximate closed-open

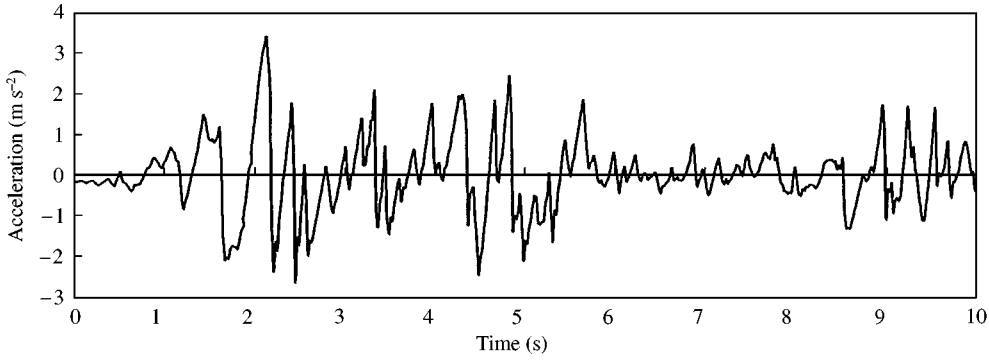

Figure 4. El Centro earthquake.

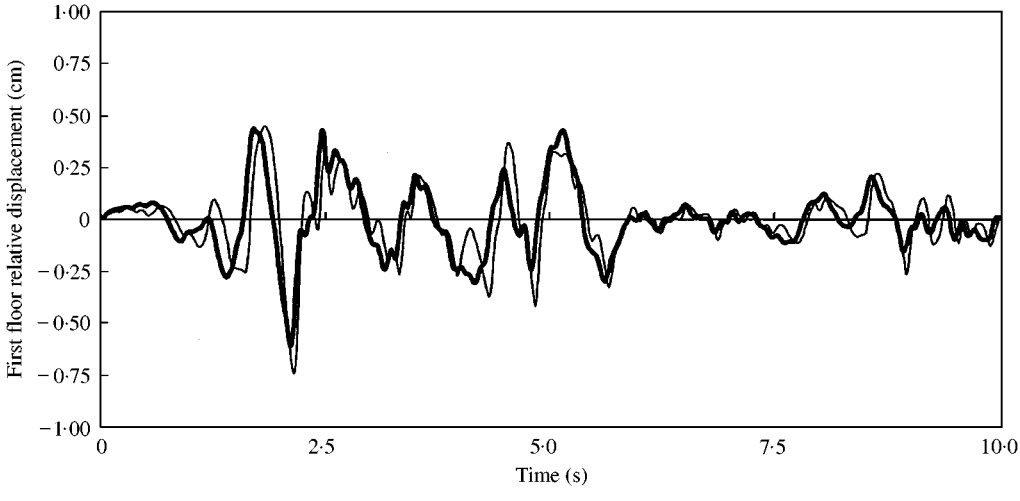

Figure 5. Relative displacements of the first floor (Standard LQR, $\alpha = 0$): ——, approximate solution; ——, optimal closed–open loop.

loop with six-step ahead prediction. Figures 5 and 6 show that the agreement between the optimal and the approximate solutions is better for the first floor than the third floor except for the maximum values.

Peak values for the storey relative displacements (x_{max}), accelerations ($\ddot{x}_{max}$) and the control forces(u_{max}) are shown in Table 1. Table 1 shows that the optimal closed–open loop control is the best in terms of the reduction is response and control force. However, it can only serve as an ideal optimal case to check the control efficiency of the other control algorithms. Numerical results also show that the approximate closed–open loop control with prediction results in smaller peak responses and control forces when compared to the closed-loop control.

Now, the relationship between the stability order α and closed-loop system matrix $\tilde{\mathbf{A}}$ will be investigated. Since the closed-loop system matrix $\tilde{\mathbf{A}} = \mathbf{A} - \frac{1}{2}\mathbf{B}\mathbf{R}^{-1}\mathbf{B}^{\mathrm{T}}\mathbf{P}$ is dependent on the stability order α through $\mathbf{P}$, as the stability order α changes, the closed-loop system matrix $\tilde{\mathbf{A}}$ and its eigenvalues will change as well. For the uncontrolled structure $\tilde{\mathbf{A}} = \mathbf{A}$ and eigenvalues of $\mathbf{A}$ for the investigated problem are obtained as 50·425i, − 50·425i, 31·102i, − 31·102i, 12·868i, − 12·868i. Since the real parts of all the eigenvalues are not negative, the

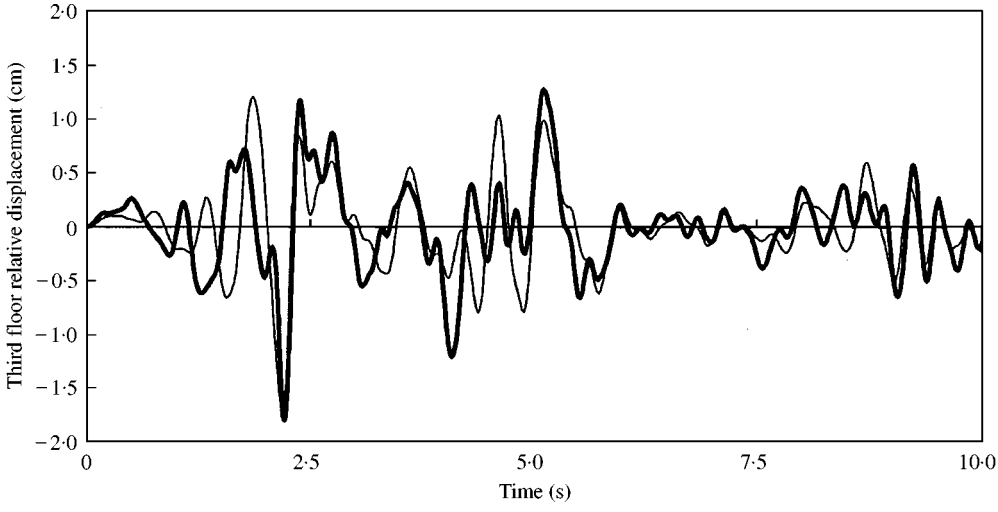

Figure 6. Relative displacements of the third floor (Standard LQR, $\alpha = 0$): ——— , approximate solution; ——— , optimal closed–open loop.

TABLE 1

Traditional LQR ($\alpha = 0$)

	x_{max} (cm)			$\ddot{x}_{max}$ (m/s^2)			u_{max} (kN)		
Storey	1	2	3	1	2	3	1	2	3
No control force	4·90	8·58	12·72	10·07	14·40	18·49	—	—	—
Closed-loop ($\mathbf{r}(t) = \mathbf{0}$)	0·91	1·85	3·05	3·07	4·88	6·18	280	223	211
Optimal closed–open loop†	0·61	0·82	1·81	2·61	3·38	4·44	167	152	192
Approximate solution									
1-step ahead prediction	0·82	1·66	2·75	2·70	4·41	5·61	278	212	195
2-step ahead prediction	0·76	1·52	2·48	2·65	4·09	4·96	285	206	182
3-step ahead prediction	0·73	1·41	2·23	2·79	3·91	4·26	283	203	173
4-step ahead prediction	0·72	1·33	2·00	3·04	3·88	3·58	275	200	167
5-step ahead prediction	0·73	1·29	1·81	3·32	3·96	3·36	264	209	166
6-step ahead prediction	0·74	1·26	1·67	3·57	4·14	3·42	253	214	175

†With *a priori* knowledge of excitation.

uncontrolled structure is not asymptotically stable. This is an obvious result for an undamped structure with no energy dissipation. Eigenvalues of the closed-loop system matrix $\tilde{\mathbf{A}}$ for $\alpha = 0, 1, 2, 3, 4, 5$ are given in Figure 7. As shown in Figure 7, the real parts of all the eigenvalues of the closed-loop system matrix $\tilde{\mathbf{A}}$ for all α values are negative. Therefore, the structure under optimal control force is asymptotically stable. It is also seen from Figure 7 that the real parts of the eigenvalues move more into the left side of the complex plane as α increases and these real parts are always less than $-\alpha$. Therefore, α can be treated as a measure of the system stability [15].

Now, the relation between α and the approximate solution of the optimal closed–open loop control is examined. As mentioned before, approximate solution for equation (27) is

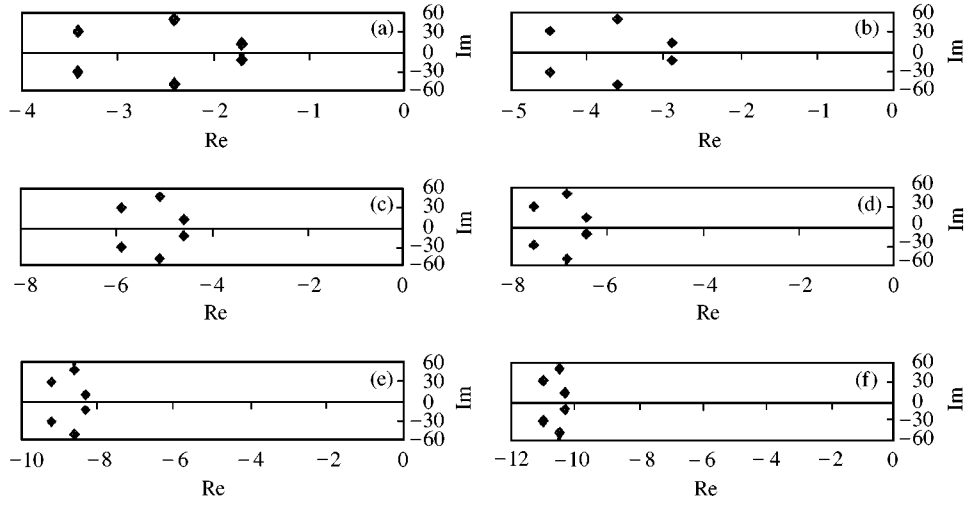

Figure 7. Eigenvalues of closed-loop system matrix $\tilde{\mathbf{A}}$ for different α values: (a) $\alpha = 0$; (b) $\alpha = 1$; (c) $\alpha = 2$; (d) $\alpha = 3$; (e) $\alpha = 4$; (f) $\alpha = 5$.

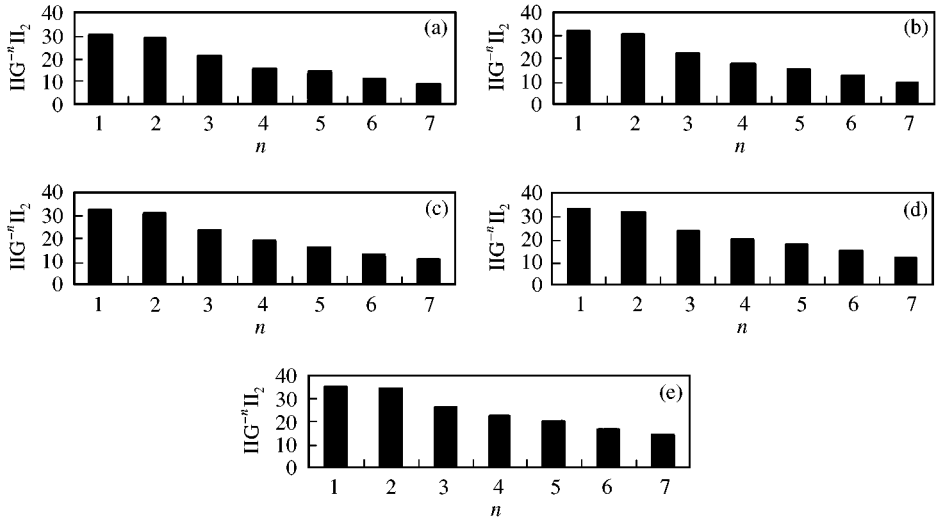

Figure 8. Variation of $\|\mathbf{S}^{-n}\|_2$ with respect to n for different α values: (a) $\alpha = 0$; (b) $\alpha = 1$; (c) $\alpha = 2$; (d) $\alpha = 3$; (e) $\alpha = 4$.

valid if $\|\mathbf{S}^{-n}\|_2$ decreases sharply with increasing n. The change of $\|\mathbf{S}^{-n}\|_2$ with respect to n is shown in Figure 8 for different α values. As shown in Figure 8, $\|\mathbf{S}^{-n}\|_2$ decreases quickly for all α values as n increases. Therefore, approximate solution of equation (27) can be obtained by predicting the near-future acceleration values of the unknown earthquake.

$\|\mathbf{S}^{-n}\|_2$ can in fact be treated as a measure of the contribution of the nth earthquake acceleration value in the exact solution. If $\|\mathbf{S}^{-1}\|_2$ is greater than $\|\mathbf{S}^{-2}\|_2$, then this means that the first earthquake acceleration value is more significant than the second earthquake acceleration value in the solution. For this purpose, the change of $\|\mathbf{S}^{-n}\|_2$ with respect to the stability order α is shown in Figure 9 for $n = 1, 2, 3, 4$. Figure 9 illustrates that the significance of each earthquake acceleration value increases as the stability of the system

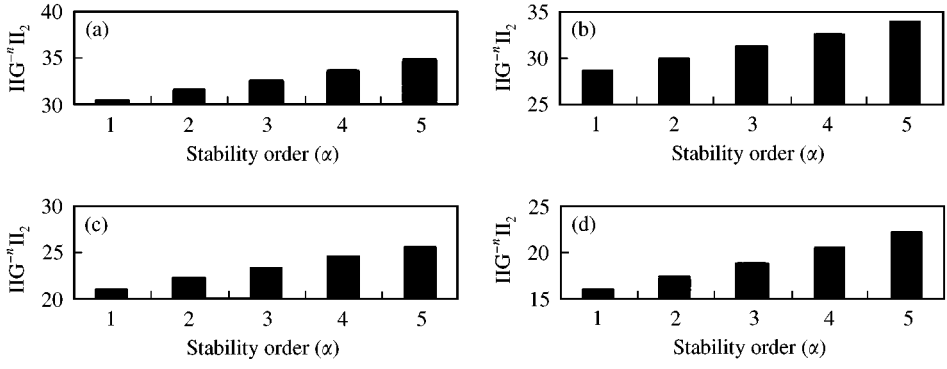

Figure 9. Variation of $\|\mathbf{S}^{-n}\|_2$ with respect to α for different n values: (a) $n = 1$; (b) $n = 2$; (c) $n = 3$; (d) $n = 4$.

TABLE 2

MLQR control ($\alpha = 1$)

	x_{max} (cm)			$\ddot{x}_{max}$ (m/s^2)			u_{max} (kN)		
Storey *Approximate solution*	1	2	3	1	2	3	1	2	3
1-step ahead prediction	0·70	1·41	2·28	2·53	4·11	4·90	294	212	191
2-step ahead prediction	0·64	1·26	2·00	2·46	3·76	4·18	305	206	176
3-step ahead prediction	0·61	1·15	1·74	2·60	3·55	3·42	304	205	164
4-step ahead prediction	0·61	1·08	1·50	2·86	3·50	2·75	296	223	157
5-step ahead prediction	0·61	1·03	1·31	3·15	3·58	2·71	284	235	179
6-step ahead prediction	0·63	1·01	1·18	3·42	3·77	2·86	273	243	209

TABLE 3

MLQR control ($\alpha = 2$)

	x_{max} (cm)			$\ddot{x}_{max}$ (m/s^2)			u_{max} (kN)		
Storey *Approximate solution*	1	2	3	1	2	3	1	2	3
1-step ahead prediction	0·59	1·18	1·86	2·33	3·79	4·24	316	214	183
2-step ahead prediction	0·53	1·03	1·57	2·24	3·41	3·44	328	207	165
3-step ahead prediction	0·51	0·93	1·30	2·38	3·18	2·62	327	229	151
4-step ahead prediction	0·51	0·85	1·07	2·67	3·11	2·13	318	248	175
5-step ahead prediction	0·52	0·81	0·89	3·04	3·18	2·21	306	262	207
6-step ahead prediction	0·54	0·79	0·78	3·36	3·37	2·39	293	269	238

increases. To be able to investigate the relationship between the system stability, prediction and the system response, maximum storey relative displacements, accelerations and the control forces of the example structure are calculated and given in Tables 2–5.

It is obvious for all α values that as the more distant-future earthquake acceleration values are predicted precisely, relative displacements decrease significantly. It is also well

TABLE 4

MLQR control ($\alpha = 3$)

	x_{max} (cm)			$\ddot{x}_{max}$ (m/s^2)			u_{max} (kN)		
Storey *Approximate solution*	1	2	3	1	2	3	1	2	3
1-step ahead prediction	0·50	0·98	1·50	2·13	3·48	3·65	338	216	173
2-step ahead prediction	0·44	0·84	1·21	2·02	3·05	2·79	351	228	154
3-step ahead prediction	0·42	0·73	0·94	2·22	2·80	1·91	350	251	164
4-step ahead prediction	0·42	0·66	0·71	2·58	2·71	1·66	340	271	195
5-step ahead prediction	0·44	0·62	0·57	2·96	2·78	1·82	327	284	227
6-step ahead prediction	0·46	0·62	0·51	3·29	2·97	2·06	313	292	259

TABLE 5

MLQR control ($\alpha = 4$)

	x_{max} (cm)			$\ddot{x}_{max}$ (m/s^2)			u_{max} (kN)		
Storey *Approximate solution*	1	2	3	1	2	3	1	2	3
1-step ahead prediction	0·42	0·82	1·22	1·94	3·17	3·18	359	223	163
2-step ahead prediction	0·36	0·68	0·92	1·88	2·70	2·26	372	246	151
3-step ahead prediction	0·34	0·57	0·66	2·09	2·42	1·33	370	270	178
4-step ahead prediction	0·35	0·51	0·45	2·45	2·32	1·32	360	284	209
5-step ahead prediction	0·37	0·48	0·36	2·84	2·38	1·55	345	303	242
6-step ahead prediction	0·40	0·48	0·35	3·19	2·61	1·95	329	311	274

known that it is rather difficult to predict the more distant-future earthquake acceleration values since the prediction error increases. However, it is seen from Tables 2–5 that there is no need to predict the more distant-future earthquake acceleration values to be able to achieve a given reduction in displacements as the system stability increases. For example, for $\alpha = 0$ and six-step ahead prediction (Table 1), maximum relative first, second and third storey displacements are 0·74, 1·26 and 1·67 cm respectively. However, for $\alpha = 3$ and one-step ahead prediction (Table 4), these displacements are 0·50, 0·98 and 1·50 cm. This shows that just one-step ahead prediction with $\alpha = 3$ is more effective than six-step ahead prediction with $\alpha = 0$ to achieve a given performance in terms of response reduction. It should be pointed out that the magnitude of the control force increases as the relative displacements fall. However, this increase is not significant. Tables 2–5 also show that the first storey accelerations increase as the number of ahead predictions increases for all α values while the increase in the second and third floor accelerations begins after the fourth-step ahead predictions. However, accelerations decrease as the stability order α increases.

5. CONCLUSIONS

Instead of the standard linear quadratic regulator (LQR) control, which is frequently employed for earthquake-excited structures, analytical solution of the modified linear

quadratic regulator (MLQR) problem including a parameter α, known in literature as system stability order, is derived in the presence of unknown seismic excitation. The derivation results in a closed–open loop control algorithm such that the active control force depends on the structure state, seismic disturbance and α. The stability order α has a contribution to the active control force in both feed-forward and feed-back terms. Numerical solution of the problem is carried out approximately by including the near-future excitation influence in the solution. In a numerical example, responses of a three-storey undamped structure are examined for different α values to investigate the relationship between the stability order α and the near-future excitation. Numerical results show that (a) the reduction in the relative displacements increases significantly for each selected α value as the more distant-future excitation is predicted precisely (it should be noted here that there is an increase in the control forces, although this increase is not significant); (b) the significance of each predicted earthquake acceleration value in the solution increases as the system stability order α is increased; therefore, a given performance in terms of the reduction in relative displacements can be achieved by predicting fewer near-future excitation values for higher values of α; (c) the storey accelerations decrease as the stability order α increases, although for a given α, accelerations increase in general especially after the fourth-step ahead predictions.

ACKNOWLEDGMENT

Support for this work from Istanbul Technical University Research Fund (Project Number: 707) is greatfully acknowledged.

REFERENCES

1. J. T. P. Yao 1972 *American Society of Civil Engineers Journal of Structural Division* **98**, 1567–1574. Concept of structural control.
2. T. T. Soong 1990 *Active Structural Control*: *Theory and Practice* Essex: Longman Scientific and Technical.
3. G. W. Housner, L. A. Bergman, T. K. Caughey, A. G. Chassiakos, R. O. Claus, S. F. Masri, R. E. Skelton, T. T. Soong, B. F. Spencer and J. T. P. Yao 1977 *ASCE Journal of Engineering Mechanics* **123**, 897–958. Structural control: past, present and future.
4. L. S. Pontryagin and P. V. Boltianski 1962 *Mathematical Theory of Optimal Processes*. Moscov: Fizmagtiz.
5. R. Bellman 1957 *Dynamic Programming*. Princeton, NJ: Princeton University Press.
6. J. N. Yang, A. Akbarpour and P. Ghaemmaghami 1987 *American Society of Civil Engineers Journal of Engineering Mechanics* **113**, 1369–1386. New optimal control algorithms for structural control.
7. J. N. Yang, Z. Li, and S. C. Liu 1992*American Society of Civil Engineers Journal of Engineering Mechanics* **118**, 1612–1630. Stable controllers for instantaneous optimal control.
8. S. F. Masri, G. A. Bekey and F. E. Udwadia 1980 in *Structural Control* Amsterdam North Holland, (H. H. E. Leipholz, editor) 471–492. On-line pulse control of tall buildings.
9. J. Rodellar, A. H. Barbat and J. M. Martin-Sanchez 1987 *American Society of Civil Engineers Journal of Engineering Mechanics* **113**, 797–812. Predictive control of structures.
10. S. K. Lee and F. Kozin 1987 in *Structural Control* (H. H. E. Leipholz, editor) 387–407. Amsterdam, Martinus Nijhoff. Bounded state control of linear structures.
11. M. Kawahara and K. Fukazawa 1989 *Structural Engineering J Earthquake Engineering* (*Proceedings. of JSCE No.* 404/*I* − 11) **6**, 179–190. Optimal control of structure subject to earthquake loading using dynamic programming.
12. H. Iemura, Y. Yamada, K. Izuna, Y. Iwasaki and S. Ohno 1990 *U.S. Workshop on Structural Control*, *Los Angeles*. Phase-Adjusted active control of structures with identification of random earthquake ground motion.

13. T. SATO and K. TOKI 1990 *Journal of Intelligent Material Systems and Structures*. **1**, 447–475. Active control of seismic response of structures.
14. U. ALDEMIR and M. BAKIOGLU 1999 13*th ASCE Engineering Mechanics Division Conference, Baltimore MD, USA*. Semiactive control of earthquake excited structures.
15. P. DORATO, C. ABDALLAH and V. CERENO 1995 *Linear Quadratic Control*. Englewood Cliffs, NJ: Prentice-Hall.
16. B. D. O. ANDERSON and J. B. MOORE 1990 *Optimal Control: Linear quadratic methods*. Englewood Cliffs, NJ: Prentice-Hall.
17. F. R. GANTMACHER 1960 *The Theory of Matrices*. Vol II, New York: Chelsea Publication Company.
18. M. BAKIOGLU and U. ALDEMIR 2001 *International Journal for Numerical Methods in Engineering* **50**, 2601–2616. A new numerical algorithm for sub-optimal control of earthquake excited linear structures.

APPENDIX A: NOMENCLATURE

$\mathbf{A}$	system matrix
$\tilde{\mathbf{A}}$	closed-loop system matrix
$\mathbf{C}$	damping matrix
H	Hamiltonian function
J	performance index
$\mathbf{K}$	stiffness matrix
$\mathbf{L}$	location matrix of controllers
$\mathbf{M}$	mass matrix
$\mathbf{P}$	Riccati matrix
$\mathbf{Q}$	weighting matrix for response
$\mathbf{R}$	weighting matrix for control
$\mathbf{U}$	control vector
$\mathbf{X}$	response vector
$\mathbf{Z}$	state vector
c_i	damping coefficient for the ith storey
h	time step
k_i	stiffness coefficient for the ith storey
m_i	mass of the ith storey
t_1	final time
u_i	control force for the ith storey
$\ddot{x}_g(t)$	earthquake ground acceleration
x_i	relative displacement for the ith storey
$\ddot{x}_i$	acceleration for the ith storey
α	stability order of the system
λ	Lagrangian vector